Article

Wide Field-of-View, High-Resolution Plastic Lens Design with Low F-Number for Disposable Endoscopy

Dongmok Kim [1], Sehui Chang [2] and Hyuk-Sang Kwon [1,*]

[1] Department of Biomedical Science and Engineering, Gwangju Institute of Science and Technology,
    123 Cheomdan-gwagiro, Buk-gu, Gwangju 61005, Korea; dongmok@gist.ac.kr
[2] Gwangju Institute of Science and Technology, School of Electrical Engineering and Computer Science,
    123 Cheomdan-gwagiro, Buk-gu, Gwangju 61005, Korea; shchangj@gm.gist.ac.kr
*   Correspondence: hyuksang@gist.ac.kr

Abstract: In the past few decades, video endoscopy has become one of the primary medical devices in diverse clinical fields for examination, treatment, and early disease diagnosis of the gastrointestinal tract. For an accurate diagnosis, an endoscopic camera offering bright and wide field-of-view images is required while maintaining its compact dimensions to enter the long, narrow, and dark tract inside of the body. Recent endoscopic lenses successfully provide wide fields-of-view and have compact sizes for the system; however, their f-numbers still remain at 2.8 or higher. Therefore, further improvement in f-numbers is required to compensate for the restricted illumination system of the endoscopic probe. Here, we present a low f-number endoscopic lens design while providing wide field-of-view and high-resolution imaging. The proposed lens system achieved a low f-number of 2.2 and a field-of-view of 140 deg. The modulation transfer function (MTF) is over 20% at 180 lp/mm, and relative illumination is more than 60% in the full field. Additionally, the proposed lens is designed for a 1/4" 5-megapixel complementary metal-oxide-semiconductor (CMOS) image sensor with a pixel size of 1.4 μm. This all-plastic lens design could help develop a high-performance disposable endoscope that prevents the risk of infection or cross-contamination with mass manufacture and low cost.

Keywords: endoscopic lens design; imaging system; disposable endoscopy; optical design; endoscope; ZEMAX

1. Introduction

Over the past few decades, endoscopy such as colonoscopy and gastroscopy has been adopted as a primary medical device in diverse clinical fields for examination, treatment, and early diagnosis of digestive diseases including cancer [1]. After the first clinical introduction of the endoscope, various types of endoscopic imaging systems, for instance, endomicroscopy with laser scanning techniques and capsule endoscopes, have been suggested. These are suggested in efforts to achieve more precise visual information from target lesions for gastrointestinal disease diagnosis.

Laser scanning microscopy-based endomicroscopes, such as multiphoton [2,3] and confocal microscopy [4,5], have the advantage of not requiring a separate biopsy process of tissue resection while observing the tissue with a high resolution at the cellular level based upon a fluorescent imaging technique. Furthermore, multimodal endoscopy based on modern biophotonics techniques has been introduced. Endoscopy capable of hyperspectral and white light imaging simultaneously [6] and the laparoscopic method adopting laser speckle contrast imaging have been established [7,8]. However, endomicroscopes based on laser scanning remain in the rudimentary stage in practice because of their limited field-of-view [9], a prerequisite of fluorescent dye, and because of their high cost [10].

On the other hand, the capsule endoscope is capable of reducing patient's discomfort caused by the insertion of the long tube connected to the outside during the examination

process with the conventional video endoscope. In addition, it enables recording observations of the entire digestive system, including the small intestine, simply by swallowing it, similar to a pill [11,12]. However, the capsule endoscope, which is a device focused in recording the digestive tract, does not offer a real-time inspection; therefore, additional examination by the conventional endoscope is still required when proactive measures such as polyp removal have to be taken. In this regard, conventional video endoscopes have been utilized as an essential type of endoscopic system in terms of a therapeutic point of view as well as diagnosis until now.

The video endoscope as an image acquisition device for diagnosing the digestive system should have a wide field-of-view to minimize blind zones and to acquire more visual information. At the same time, a brighter lens with larger image sensor is preferred in order to obtain images capable of discriminating abnormality in the gastrointestinal tract under dim light environment inside of the body, which is caused by the limited illumination system. Hence, modern video endoscopy requires a lens that can support a wide field-of-view, a low f-number, and high resolution to achieve high-quality imaging performance.

In recent years, several studies of wide field-of-view endoscopic lens design have been demonstrated. Dallaire and Thibault proposed a wide-angle endoscopic lens by introducing a foveated imaging technique [13]. Coral and Leblebici presented a miniaturized multi-camera system inspired by insect eyes for wide field-of-view endoscopic imaging [14]. Lin et al. introduced a front and panoramic side-view endoscopic lens system by adopting a rotating lens [15]. However, most designs above remain in the f-number range from 2.8 to 6.

In terms of miniature lens design, the lens design with a small form factor capable of resolving more than 10-megapixels, which is applicable for smartphone cameras as well as endoscopic use, has been proposed [16,17]. However, this high-resolution miniature lens cannot provide a wide field-of-view at the same time while maintaining a low f-number.

Conventional video endoscopes are exposed to the risk of infection and cross-contamination from reuse of the system, so the used endoscopes require a high level of cleaning, disinfection, and sterilization [18]. In this regard, a disposable endoscopic lens is required for preventing infection or cross-contamination [19,20].

Here, we present a low f-number lens design for a video endoscope system, which provides high-resolution imaging with a wide field-of-view. A low f-number of 2.2 of the proposed endoscopic lens allows us to obtain bright images in spite of the restricted illumination system. In the design process, the wide field-of-view and compact size of the lens structure are also considered to meet the fundamental requirements for endoscopic use. We designed the lens system using only plastic materials for disposable use in order to prevent risk of infection or cross-contamination from reuse of the endoscopic system. The design of all plastic lens systems with high imaging performance is quite challenging because of the relatively low refractive index of plastics compared to common glass materials. The optimization process with aspheric surfaces successfully overcomes the challenges with plastic materials, and eventually, all plastic lens systems offer various advantages such as lightweight, mass production, and cost-effectiveness.

This paper is composed of the following sections. Section 2 describes the design concept and method. Section 2.1 elaborates the design concept and the specifications of the lens. Detailed lens design method and optimization process are described in Section 2.2. The performance of the optimized lens system is evaluated mainly in terms of aberration plots, modulation transfer function (MTF), and relative illumination in Section 3. The result of this study is discussed in Section 4, and the conclusion is presented in Section 5.

2. Materials and Methods

2.1. Design Concept

The main focus of this study is to design a low f-number lens while offering a wide field-of-view with high-resolution imaging. The compact size of an endoscopic system limits supplementary illumination; thus, it requires a lens system with low f-number in

order to overcome the dim environment. In this regard, we pursue designing a endoscopic lens system with a low f-number of 2.2 while achieving competitive values in other specifications such as field-of-view, MTF, and relative illumination.

The f-number of the optical system is defined as the ratio of effective focal length and the entrance pupil diameter, EFL/EPD. The irradiance of the lens system is proportional to $1/f\text{-}number^2$ [21,22], which means that a lens with an f-number of 2.2 can obtain 2.53 times brighter images than the one with an f-number of 3.5 and 1.62 times brighter image than the other with f-number 2.8, the typical value of recently proposed endoscopic lens designs [13]. Hence, in identical dim lighting environment and physical dimensions of the lens, minimizing a lens' f-number is important to enhance its optical performance. Moreover, a wide field-of-view is also required to obtain more diagnostic information; therefore, the target value was set to have 140 deg of field-of-view at 15 mm working distance.

The total length of the system from the first lens component to the image plane was set to 10 mm with consideration of the conventional endoscope system. The lens diameter was targeted under 5 mm to guarantee enough space for other instruments such as an irrigation channel, a suction channel, and a biopsy channel [23]. Aspheric surfaces are introduced in order to efficiently compensate for the generated optical aberrations of the lens. All lenses adopted plastic materials (e.g., APL5014CL and OKP-A2) to ensure the manufacturability of the aspheric lenses. The lens was designed to obtain more than 0.6 of relative illumination at full fields to avoid darkening at the peripheral region of the image.

The sensor size of the imaging system determines the amount of light to form an image. With larger sensors utilized, the larger pixels in the sensor collect more lights, which means that a large image sensor has more advantages than a small sensor for high-quality imaging. Therefore, a size of 1/4″ for the image sensor was selected in this study. The lens system was designed for a 1/4″ 5-megapixel color CMOS image sensor from OmniVision [24]. The image area of the CMOS sensor is 3684 μm × 2763 μm, and its diagonal is 4605 μm. Accordingly, the half image height is set to 2302 μm, and the pixel size is 1.4 μm × 1.4 μm. Since an RGB color sensor with Bayer filter comprises 2 × 2 = 4 sensing pixels, it is calculated to have a spatial resolution two times lower than the monochromatic image sensor. Therefore, the spatial frequency of the lens with the RGB color image sensor is given by [25]

$$\text{Spatial frequency (lp/mm)} = \frac{1}{4 \times \text{pixel size (mm)}} \tag{1}$$

The MTF graph is referred to as a standard of the overall image quality of the imaging system. To achieve the appropriate image quality of the lens, the MTF should be over 0.2 at 178.6 lp/mm. Therefore, in this study, the MTF was set over 0.2 at 180 lp/mm. The design specifications of the proposed endoscopic lens are shown in Table 1.

Table 1. Design specifications.

Item	Specifications
f-number	2.2
Field-of-view	140 deg
Working distance	15 mm
Half image height	2.3 mm
Total track length	<10 mm
Relative illumination	>0.6
MTF	>0.2 at 180 lp/mm

2.2. Design Method

An extensive patent search was conducted to select the initial design structure. Several characteristics such as wide field-of-view, low f-number, and compact dimensions were

mainly focused on the initial structure search process, which was in conjunction with the target specifications for endoscopic use. The selected lens design as an initial structure was originally designed for automotive or surveillance camera systems, which require system miniaturization, wider field-of-view, and bright lens in a dim environment [26].

The initial design had an f-number of 2.5, a field-of-view of 120 deg, and a total track length of approximately 23.16 mm. The selected optical system had total four lenses, which consisted of one plastic lens and three glass lenses, excluding the IR (infrared) filter, and its third, fourth, and fifth surfaces consisted of even aspheres.

The aperture stop of the initial design was optimized during the design process to have an image space f-number of 2.2, which is a relatively large aperture stop for endoscopic use. The target field was initially divided into four field values according to the real image height of 2.3 mm, which meet the half image height 2302 μm of the selected 1/4″ 5-megapixel image sensor, and later, we changed field data from the real image height to angle to ensure the optical performance of the system in terms of its half field-of-view from 0 deg to 70 deg (0, 30, 45, and 70 deg). The wavelength was set in the visible range of F, d, and C (486.1, 587.6, and 656.3 nm).

For endoscopic use, lens materials of the proposed lens system were chosen in plastic materials due to its advantages, including cost-effectiveness, lightweight, and mass production. The injection molding techniques can be utilized for plastic lens fabrication, and once the initial platform is established, then it is available not only to mass produce the lenses at a low cost but also to mold the aspheric surfaces readily. Despite its limited range of material selection in plastics and its relatively low refractive index compared to glass materials, the other characteristics mentioned above are sufficiently attractive for endoscopic objective lens fabrication. In this study, only two plastic materials were adopted to design the lens system while compensating for the chromatic aberrations. The first, second, and third lenses used APL5014CL, which is a crown-like plastic material with a refractive index of 1.54 and an Abbe number of 56.0. APL5014CL, a cyclo-olefin copolymer material, is suitable for manufacture of the lens by ensuring low water absorption, low autofluorescence, high chemical resistance [27], and relatively high refractive index. The material for the fourth lens was OKP-A2. It is a flint-like material with a refractive index of 1.66 and an Abbe number of 20.4 and has a relatively high dispersion compared to APL5014CL.

The development of fabrication techniques such as diamond turning and injection molding has introduced advanced aspheric surfaces, allowing lens designers to effectively handle optical aberrations. Aspheric surfaces are mainly adopted for complex lens systems, which requires a large field angles and low f-number [25]. In the design process, all surfaces were set to even asphere to reduce the generated aberrations for high imaging quality. The aspheric surface profile is defined by the following equation [28]:

$$Z = \frac{ch^2}{1 + \sqrt{1 - (1 + \kappa)c^2 h^2}} + \alpha_4 h^4 + \alpha_6 h^6 + \alpha_8 h^8 + \cdots + \alpha_n h^n \,, \qquad (2)$$

where Z is the surface sag, c is the curvature of the surface, h denotes the radial distance from the vertex, κ is the conic constant of the surface, and α_n indicates the nth-order aspheric coefficients. The conic parameter κ is likely to offset the 4th-order term, and there was no significant improvement in further optimizations with a variable of the conic parameter in the design process [25]. Therefore, we decided to be the 4th-order term as a variable during the optimization process, and the conic parameter κ was fixed to 0. In this study, only 4-, 6th-, 8th-, and 10th-order aspheric coefficients were used to optimize the system to reduce the manufactural complexity. Table 2 shows the lens data and the aspheric coefficients of the proposed lens system.

Table 2. Lens data of the optimized system.

Surface	Radius (mm)	Thickness (mm)	Material	Aspheric Coefficient			
				4th	6th	8th	10th
L1	12.190	0.400	APL5014CL	-0.012	1.182×10^{-3}	-7.133×10^{-5}	1.420×10^{-6}
	1.450	1.777		-0.022	0.027	-0.016	4.255×10^{-3}
Stop	Infinity	0.875					
L2	15.480	1.640	APL5014CL	-0.014	5.225×10^{-3}	-8.088×10^{-3}	1.552×10^{-3}
	-2.190	0.050		5.254×10^{-3}	-2.523×10^{-3}	6.324×10^{-4}	-2.257×10^{-4}
L3	4.520	1.850	APL5014CL	1.274×10^{-3}	-7.698×10^{-4}	1.678×10^{-5}	-3.472×10^{-5}
	-2.590	0.045		6.091×10^{-3}	-1.95×10^{-4}	2.818×10^{-4}	4.692×10^{-6}
L4	-2.450	0.400	OKP-A2	6.773×10^{-3}	1.374×10^{-3}	3.575×10^{-5}	1.035×10^{-4}
	57.130	2.600		4.012×10^{-3}	7.018×10^{-4}	-3.147×10^{-4}	8.248×10^{-5}
IR filter	Infinity	0.500	BK7				
	Infinity	0.550					
Image	Infinity						

The optimization process is conducted by varying design parameters such as air space, lens thickness, radius of curvature, and aspheric coefficient. Then, it is repeated until the optimal performance is achieved by monitoring the ray fan aberration graph and the MTF graph. The optimization process was performed with ZEMAX optical design software by specifying certain constraints and targets to satisfy the design specifications such as lens diameter, total length of the system, image height, and so forth. For the default merit function, root mean square (RMS) and wavefront are set as type and data criteria of optimization function, respectively, and the reference point is set to the centroid. The Gaussian quadrature was set as a pupil integration method. The damped least square method was used in local optimization. Final tuning of the system was done with modulation of the variables by running through the trial-and-error process. In addition, appropriate vignetting was intentionally utilized to improve overall image quality in the lens design process, with some loss of relative illumination in this process, but it is still above the target requirement of a relative illumination of 0.6. The final optical layout of the optimized lens system is shown in Figure 1. Each color of the layout represents different field angles (0, 30, 45, and 70 deg).
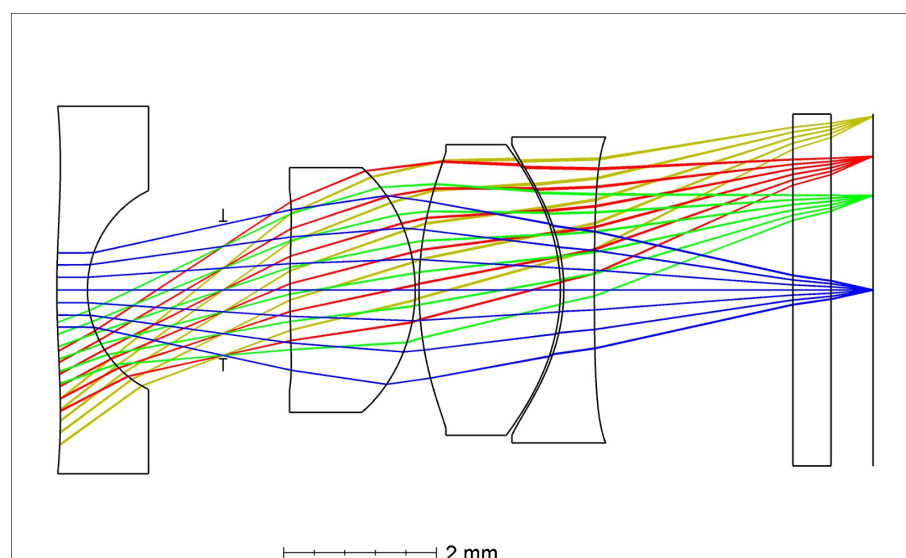
Figure 1. Optical layout of the optimized system.

3. Results

The optical performance of the proposed system was analyzed using ZEMAX optical design software. The specifications of the optimized system met the overall system requirements. The final specifications of the optimized lens are shown in Table 3.

Table 3. Specifications of the optimized system.

Item	Target	Result
f-number	2.2	2.2
Field-of-view	140 deg	140 deg
Working distance	15 mm	15 mm
Half image height	2.3 mm	2.3 mm
Total track length	<10 mm	10.68 mm
Relative illumination	>0.6	>0.68
MTF at 180 lp/mm	>0.2	>0.2

The optimized lens has EFL = 2.32577 and EPD = 1.05717, and therefore, an f-number of 2.2. The relatively low f-number of the optimized system allows for the image sensor to collect sufficient light for high-quality imaging.

The MTF graph of the proposed lens system is shown in Figure 2. The MTF values of every field (0, 30, 45, and 70 deg) show more than 0.2 at 180 lp/mm, which indicates that the optimized system offers sufficient imaging quality in spite of the adoption of a large 1/4″ 5-megapixel color CMOS image sensor.
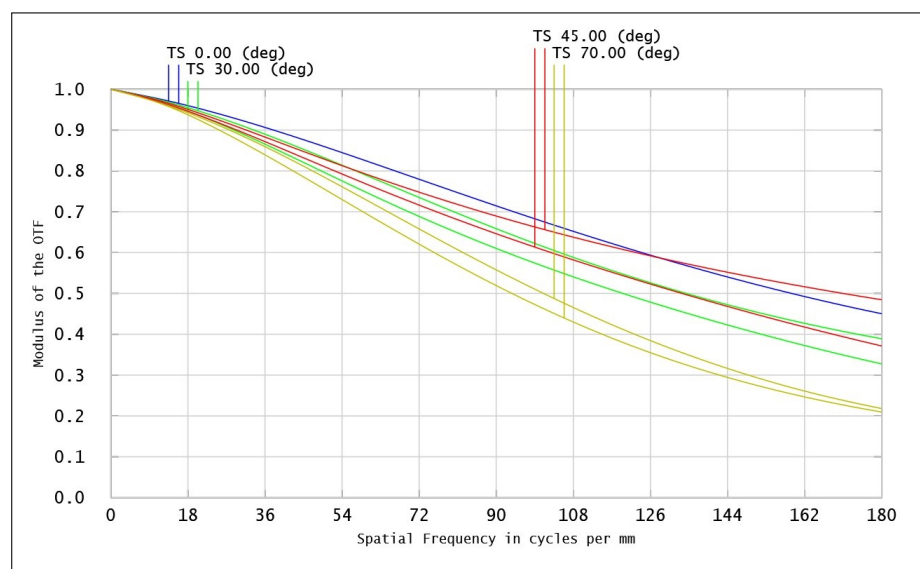

Figure 2. Modulation transfer function (MTF) of the optimized system.

The overall optical aberrations of the lens system can be evaluated by the ray fan plot shown in Figure 3. As the aberration curve of the ray fan plot gets closer to the x-axis, the aberration of the optical system decreases. The ray fan plot shows that the optimized system greatly compensated for the optical aberrations.

Figure 4 presents the field curvature and distortion of the proposed lens system. At 70 deg, the maximum F-Tan (Theta) distortion is 65% and the maximum SMIA-TV (Standard Mobile Imaging Architecture-Television) distortion is −27.57%. Distortion deforms the shape of the edges of the image, but it does not affect the resolution of the image. In the typical design process for widening the optical fields in restricted physical dimensions, distortion is unavoidable. In this study, it was corrected naturally during the entire optimization process, since the additional image processing can be adopted to compensate for the distortion if the sufficient image resolution is guaranteed [29].
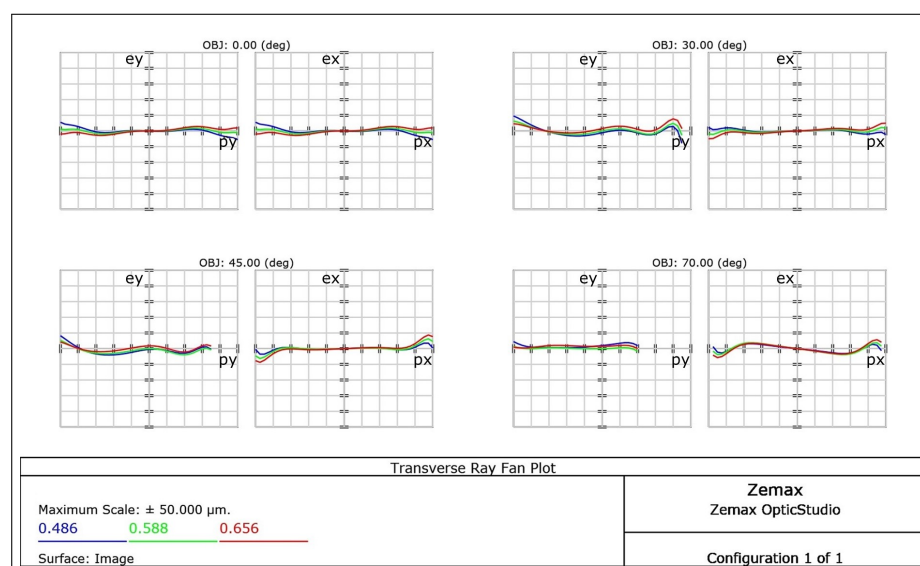
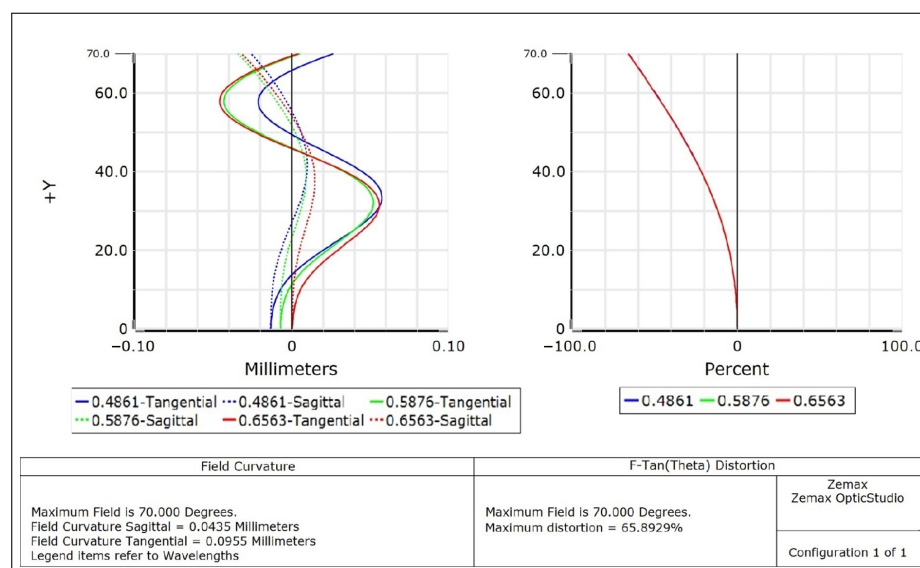**Figure 3.** Ray fan plot of the optimized system.

Figure 4. Field curvature and distortion of the optimized system.

The lateral color of the proposed system is shown in Figure 5. Based on the center wavelength of 587.6 nm, all wavelengths are nearly close to the diffraction limit in the entire fields. Considering that the proposed lens system is composed of only 4 lenses using 2 plastic materials, its optical performance is adequate for endoscopic use. Figure 6 depicts the spot diagram of the optimized system. The Airy disk radius is 1.662 μm at a wavelength of 587.6 nm, and the largest RMS radius is 3.453 μm at full field, 70 deg.

Figure 7 represents the relative illumination. In general, the image gets darker toward the peripheral area compared to the center of the image because of the different light amounts arriving in the image plane. The relative illumination of the optimized lens system is more than 0.68 even at its full field of 70 deg, which clearly shows that the illumination for the image is sufficient at all fields.
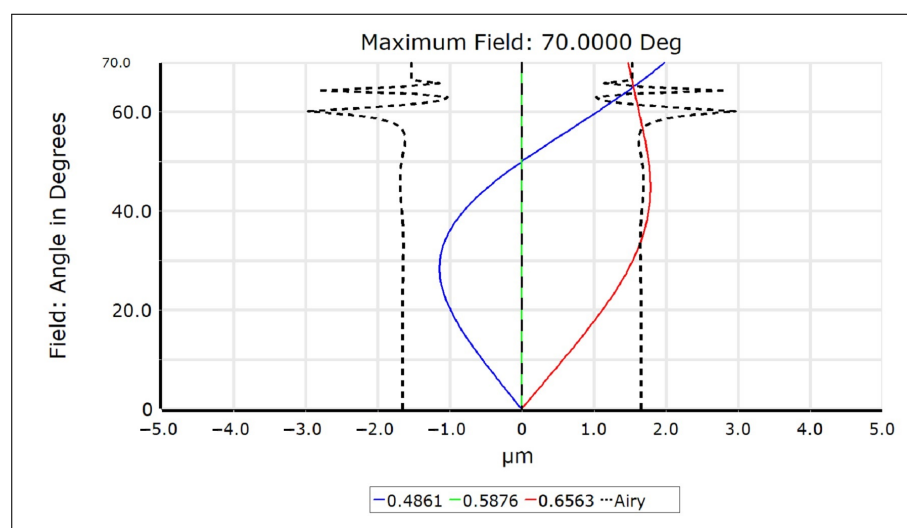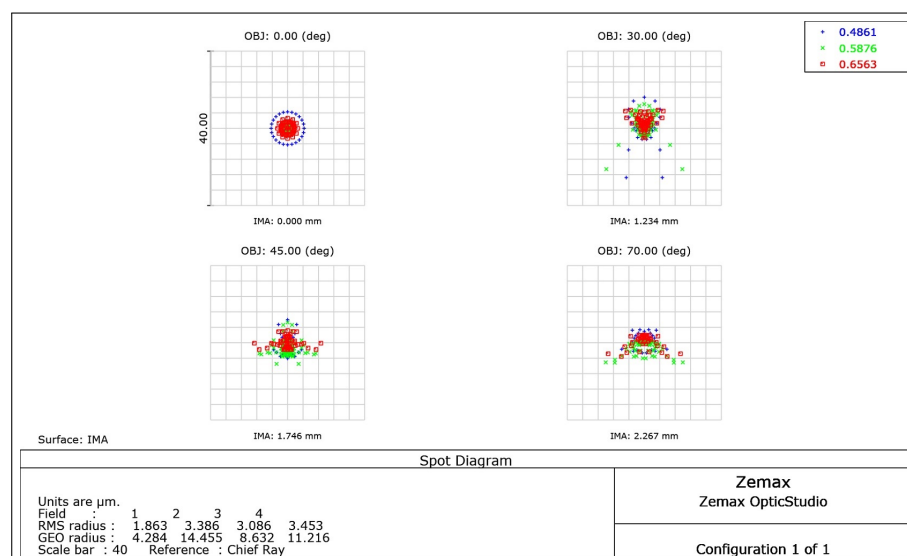
Figure 5. Lateral color of the optimized system.

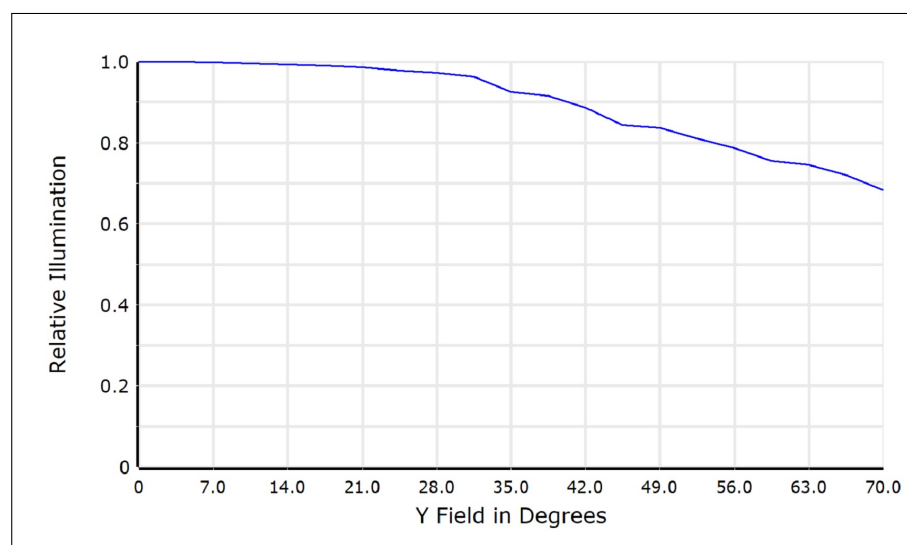**Figure 6.** Spot diagram of the optimized system.

Figure 7. Relative illumination of the optimized system.

Tolerance analysis was performed in the final design by using a built-in tolerance function in Zemax software. The tolerancing parameters are listed in the Table 4. The tolerancing requirement was set such that the geometric MTF average did not fall below 0.2 for a spatial frequency of 180 lp/mm. Then, we ran the Monte Carlo analysis 100 times. The nominal geometric MTF average value was 0.205, and the mean value was 0.173, which is acceptable for lens fabrication [25].

The f-number, field-of-view, resolution, lens diameter, and number of elements are compared with previous disposable endoscopic lens design studies in Table 5.

Table 4. Fabrication tolerances of the optimized system.

Item	Tolerances
Surface tolerances	
Radius	± 1 fringe
Thickness	± 0.005 mm
Tilt X	± 0.05 deg
Tilt Y	± 0.05 deg
S+A Irregularity	$\pm 0.5\,\lambda$
Element tolerances	
Decenter X	± 0.003 mm
Decenter Y	± 0.003 mm
Tilt X	± 0.05 deg
Tilt Y	± 0.05 deg
Index tolerances	
Index	± 0.001
Abbe %	± 1

Table 5. Performance comparison.

Item	Wippermann et al., [19]	Shim et al., [20]	This Work
f-number	4	3.5	2.2
FOV(deg)	110	110	140
Resolution (pixels)	3 MP (2048 × 1536)	0.9 MP (1280 × 720)	5 MP (2592 × 1944)
Diameter (mm)	3	3.1	5
No. of elements	3	4	4

4. Discussion

In this study, we designed a low f-number 2.2 lens with a wide field-of-view 140 deg for a high-resolution endoscope, which is 2.53 times and 1.62 times brighter than f-numbers 3.5 and 2.8, respectively. The relatively low f-number of the proposed lens enables bright images in spite of the limited illumination source of the endoscope system. The proposed lens system consists of only 4 lenses with plastic materials that are suitable for mass production and disposable use. Moreover, the introduction of a limited number of aspheric terms can not only correct the optical aberrations sufficiently but also enhance manufactural efficiency by avoiding extremely complexed surface forms. The optimized system has a total track length of approximately 10 mm with a small diameter of 5 mm and adopts a 1/4″ 5-megapixel CMOS image sensor with a pixel size of 1.4 μm. The MTF value of the system over 0.2 at 180 lp/mm indicates that the presented lens can provide high-resolution imaging. The relative illumination is more than 0.68 at the full field, which means that the bright images can be obtained without darkening even at the edge of the image.

In a wide field-of-view lens system, the distortion is unavoidable and it is challenging to mitigate the distortion in the design process. To compensate for the distortion, adopting digital image processing, which corrects distortion in real-time by using graphics hardware,

can be one of the solutions. To achieve low f-number, in general, large diameter lens elements are required for the large aperture. Moreover, it is challenging to design the system under restricted conditions such as limited material selection and compact space while maintaining a wide field and high-resolution. For this reason, the dimension of the lens system was designed to be slightly larger than previous disposable endoscopic lens designs. However, the dimension of the lens system is sufficient for endoscopic application.

5. Conclusions

The wide field-of-view, high-resolution plastic lens design with low f-number has been presented for the video endoscope system. The proposed lens system not only allows for bright, wide, and high-resolution endoscopic images but also is cost-effective with mass production. An all-plastic lens design is also possible to be applied in disposable endoscopes, preventing infection or cross-contamination. The proposed design still leaves room for improvement in overall optical performance by replacing the lens materials with a higher refractive index with additional optimization processes in future work. In addition, aside from its application in the endoscope, it can also be applied as an initial design to surveillance and automotive cameras that require wide field-of-view and bright lenses.

Author Contributions: Conceptualization, D.K.; methodology, D.K. and S.C.; software, D.K. and S.C.; validation, D.K. and S.C.; investigation, D.K. and S.C.; resources, D.K.; data curation, D.K.; writing—original draft preparation, D.K.; writing—review and editing, D.K., S.C. and H.-S.K.; visualization, D.K.; supervision, H.-S.K.; project administration, H.-S.K.; funding acquisition, H.-S.K. All authors have read and agreed to the published version of the manuscript.

Institutional Review Board Statement: Not applicable.

Informed Consent Statement: Not applicable.

Data Availability Statement: The data presented in this study are available upon request from the corresponding author.

Conflicts of Interest: The authors declare no conflict of interest.

References

1. Lambert, R. Prevention of gastrointestinal cancer by surveillance endoscopy. *EPMA J.* **2010**, *1*, 473–483. [CrossRef] [PubMed]
2. Göbel, W.; Kerr, J.N.D.; Nimmerjahn, A.; Helmchen, F. Miniaturized two-photon microscope based on a flexible coherent fiber bundle and a gradient-index lens objective. *Opt. Lett.* **2004**, *29*, 2521–2523. [CrossRef] [PubMed]
3. Akhoundi, F.; Qin, Y.; Peyghambarian, N.; Barton, J.K.; Kieu, K. Compact fiber-based multi-photon endoscope working at 1700 nm. *Biomed. Opt. Express* **2018**, *9*, 2326–2335. [CrossRef] [PubMed]
4. Yang, L.; Wang, J.; Tian, G.; Yuan, J.; Liu, Q.; Fu, L. Five-lens, easy-to-implement miniature objective for a fluorescence confocal microendoscope. *Opt. Express* **2016**, *24*, 473–484. [CrossRef] [PubMed]
5. Zaman, M.A.; Büyükalp, Y. Design of a high numerical aperture achromatic objective lens for endomicroscopy. *Opt. Eng.* **2019**, *58*, 075101. [CrossRef]
6. Yoon, J.; Joseph, J.; Waterhouse, D.J.; Luthman, A.S.; Gordon, G.S.D.; Pietro, M.D.; Januszewicz, W.; Fitzgerald, R.C.; Bohndiek, S.E. A clinically translatable hyperspectral endoscopy (HySE) system for imaging the gastrointestinal tract. *Nat. Commmun.* **2019**, *10*, 1902. [CrossRef] [PubMed]
7. Potapova, E.V.; Seryogina, E.S.; Dremin, V.V.; Stavtsev, D.D.; Kozlov, I.O.; Zherebtsov, E.A.; Mamoshin, A.V.; Ivanov, Y.V.; Dunaev, A.V. Laser speckle contrast imaging of blood microcirculation in pancreatic tissues during laparoscopic interventions. *Quantum Electron.* **2020**, *50*, 33–40. [CrossRef]
8. Zheng, C.; Lau, L.W.; Cha, J. Dual-display laparoscopic laser speckle contrast imaging for real-time surgical assistance. *Biomed. Opt. Express* **2018**, *9*, 5962–5981. [CrossRef] [PubMed]
9. Bumstead J.R.; Park, J.J.; Rosen, I.A.; Kraft, A.W.; Wright, P.W.; Reisman, M.D.; Côté, D.C.; Culver, J.P. Designing a large field-of-view two-photon microscope using optical invariant analysis. *Neurophotonics* **2018**, *5*, 1–20. [CrossRef] [PubMed]
10. Jerome, W.G.; Price, R.L. *Basic Confocal Microscopy*, 2nd ed.; Springer: Cham, Switzerland, 2018; pp. 191–192.
11. Chang, S.; Kim, D.; Kwon, H.-S. Compact wide-angle capsule endoscopic lens design. *Appl. Opt.* **2020**, *59*, 3595–3600. [CrossRef] [PubMed]

12. Han, P.; Tseng, Y.-C.; Tsai, C.-M. Wide field of view lens design with uniform image illumination in capsule endoscope system. *Microsyst. Technol.* **2018**, 1–8.
13. Dallaire, X.; Thibault, S. Design of a foveated wide-angle endoscopic lens. *Opt. Eng.* **2016**, *55*, 1–8. [CrossRef]
14. Cogal, O.; Leblebici, Y. An insect eye inspired miniaturized multi-camera system for endoscopic imaging. *IEEE Trans. Biomed. Circuits Syst.* **2017**, *11*, 212–224. [CrossRef] [PubMed]
15. Lin, C.-H.; Hsiao, L.-J.; Hsaio, J.-T.; Lin. H.Y. Front view and panoramic side view videoscope lens system design. *Appl. Opt.* **2014**, *53*, H146–H152. [CrossRef] [PubMed]
16. Kose, T.; Ben-Mrad, R. Optical design of a 2× zoom lens for miniature imaging systems. *Opt. Eng.* **2019**, *58*, 085107. [CrossRef]
17. Chen, P.; Gao, X. Optical design of the 13 mega-pixels mobile phone camera. In Proceedings of the 2016 3rd International Conference on Materials Engineering, Manufacturing Technology and Control, Taiyuan, China, 27–28 February 2016; pp. 835–840.
18. Kovaleva, J.; Peters, F.T.M.; van der Mei, H.C.; Degener, J.E. Transmission of infection by flexible gastrointestinal endoscopy and bronchoscopy. *Clin. Microbiol. Rev.* **2013**, *26*, 231–254. [CrossRef] [PubMed]
19. Wippermann, F.C.; Beckert, E.; Dannberg, P.; Messerschmidt, B.; Seyffert, G. Disposable low-cost video endoscopes for straight and oblique viewing direction with simplified integration. In *Design and Quality for Biomedical Technologies III, Proceedings of the SPIE BiOS, San Francisco, CA, USA, 23–28 January 2010*; International Society for Optics and Photonics: Bellingham, WA USA, 2010; Volume 7556, pp. 25–34.
20. Shim, D.; Yeon, J.; Yi, J.; Park, J.; Park, S.N.; Lee, N. A wide-angle camera module for disposable endoscopy. *Opt. Rev.* **2016**, *23*, 596–600. [CrossRef]
21. Pedrotti, F.L.; Pedrotti, L.M.; Pedrotti, L.S. *Introduction to Optics*, 3rd ed.; Cambridge University Press: Cambridge, UK, 2017; pp. 70–71.
22. Chabay, R.W.; Sherwood, B.A. *Matter and Interactions*, 4th ed.; Wiley: Hoboken, NJ, USA, 2015; p. 978.
23. Khanicheh, A.; Shergill, A.K. Endoscope design for the future. *Tech. Gastrointest. Endosc.* **2019**, *21*, 167–173. [CrossRef]
24. OmniVision Technologies, Co. Available online: https://www.ovt.com/sensors/OV5695 (accessed on 14 July 2020).
25. Sun, H. *Lens Design: A Practical Guide*; CRC Press: Boca Raton, FL, USA, 2017; pp. 117–118. 228–232. 324–325.
26. Song, S.H. Optical System for Surveillance Camera Using Aspherical Surface. KR Patent Application 20050118139, November 2005.
27. Prada, J.; Cordes, C.; Harms, C.; Lang, W. Design and Manufacturing of a Disposable, Cyclo-Olefin Copolymer, Microfluidic Biosensor. *Proceedings* **2018**, *2*, 810. [CrossRef]
28. Schaub, M.; Schwiegerling, J.; Fest, E.; Shepard, R.H.; Symmons, A. *Molded Optics: Design and Manufacture*, 1st ed.; CRC Press: Boca Raton, FL, USA, 2011; p. 24.
29. Bax, M.R.; Shahidi, R. Real-time lens distortion correction: Speed, accuracy and efficiency. *Opt. Eng.* **2014**, *53*, 113103. [CrossRef]